Proceeding of the IEEE
International Conference on Robotics and Biomimetics
Dali, China, December 2019

Study on Autonomous Hovering of the Spherical Underwater Robot Based on Fuzzy PD Controller

Jian Guo, *Member*, *IEEE*, Chunying Li, and Shuxiang Guo, Senior *Member*, *IEEE*

Abstract— **To make the movement of the spherical underwater robot more stable and easier to control, it is necessary to design a controller that can hover autonomously. According to the dynamic equation, we solved the transfer function of the spherical underwater robot in the dive process. Next, we designed the fuzzy PD controller which was easy to control, nonlinear and automatically adjustable. We used Simulink to build the hover motion simulation model for the spherical underwater robot, including using fuzzy PD controller and without fuzzy PD controller, and we carried out the comparative experiments of two simulation models. Then we applied the fuzzy PD controller to the hover motion of the spherical underwater robot, and carried out hover motion experiments. The experimental results showed that the fuzzy PD controller had better performance, and improved the stability of hover motion of the spherical underwater robot.**

Index Terms - The spherical underwater robot. Fuzzy PD controller. Hover motion.

I. INTRODUCTION

The underwater robot can be adapted to a variety of complex tasks and underwater working environments, and has good movements performance. In recent years, therefore, countries have increased their research investment in underwater robots, and have developed various robots to meet the mission requirements in different environments[1, 2].

The underwater robot will certainly have broad application prospects in the development and utilization of the ocean. The development of marine resources will become an important development direction for human beings[3]-[5]. In recent years, Theseus AUV, designed by Canada, can be used for underwater investigations such as remote investigation and remote hunting; 8A-4 unmanned remote submersible, jointly developed by Harbin Engineering University and Huazhong University of Science and Technology, can complete automatic directional depth and various types of work functions; but the above robots have large volume, high noise, poor concealment, etc., and can only work underwater[6]. Based on the above considerations, our laboratory has developed an underwater robot with two modes of motion. The robot can realize multi-degree of freedom movement in water, small volume and low noise[7]-[9]. It can be used for the development of uninhabited islands and the induction of fish for the benefit of mankind.

The dynamics model of most robots is difficult to determine and has the characteristics of strong coupling and nonlinearity. So it is difficult to adjust the control gain well under water. Therefore, it is necessary to design a control system with self-adjusting ability. The control methods currently used mainly include adaptive control, neural network control and fuzzy control. Since the mathematical model of the robot is not available, the coupling of degrees of freedom is difficult to describe[10]. And considering the time-varying behavior of underwater robot motion and the complexity and uncertainty of the environment[11]. The spherical underwater robot we used in this paper is nonlinear. So we use fuzzy PD controller to make the controller more flexible and adaptable.

This paper is organized as follows. The main work of Sect. 2 analyzes the underwater dynamics model of spherical underwater robot. The main work of the Sect. 3 completes the design of underwater fuzzy PD controller and the robot hover motion analysis. The main work of the Sect. 4 mainly completes underwater experiments and analyzes the experimental results. Finally, the conclusions and future work are pointed in Sect. 5.

II. SOLVING TRANSFER FUNCTION FOR THE SPHERICAL UNDERWATER ROBOT

A. Coordinate Transformation of Dynamic Equation

The coordinate system of the spherical underwater robot under water is shown in Fig. 1. E is the origin, Eε and Eη axes are set on a horizontal plane. And The direction of Eε indicates the main heading of the spherical underwater robot. The Eζ axis is oriented in the direction of the center of the earth. The inertial coordinate system satisfies the right-hand rule. The origin O of the motion coordinate system represents a point on the robot body, and the vertical axis Ox is parallel to the body and points to the front of the robot. The horizontal axis Oy is parallel to the base surface and points to the starboard side. The vertical axis Oz points to the bottom of the robot[12]-[14].

We decompose the underwater motion of the spherical underwater robot into two plane motions, horizontal and vertical. The horizontal movement mainly studies the maintenance and change of the robot's heading. Vertical motion mainly changes the depth of the robot's dive. The

*Research supported by National Natural Science Foundation of China (61703305), Key Research Program of the Natural Science Foundation of Tianjin (18JCZDJC38500) and Innovative Cooperation Project of Tianjin Scientific and Technological (18PTZWHZ00090).

Jian Guo is with the Tianjin Key Laboratory for Intelligent Robot Laboratory, Tianjin University of Technology, Tianjin 300384, China (e-mail: jianguo@tjut.edu.cn).

Chunying Li is also with the Tianjin Key Laboratory for Intelligent Robot Laboratory, Tianjin University of Technology, Tianjin 300384, China (e-mail: 1297596414@qq.com).

Shuxiang Guo is with the Tianjin Key Laboratory for Intelligent Robot Laboratory, Tianjin University of Technology, Tianjin 300384, China and also with the Department of Intelligent Mechanical Systems Engineering, Faculty of Engineering, Kagawa University, Takamatsu 7610396, Japan (corresponding author phone: +86-151-0223-1710; e-mail: guo@eng.kagawa-u.ac.jp).

978-1-7281-6321-5/19//$31.00 ©2019 IEEE

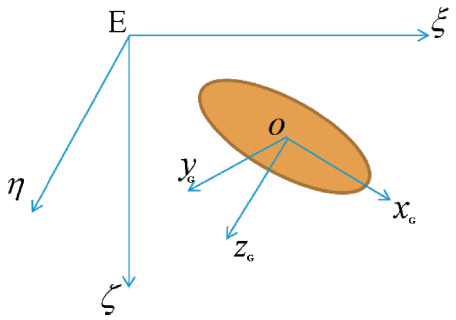

Fig. 1 System structure diagram of the spherical underwater robot.

$$
\begin{aligned}
X &= m\left[\dot{u}-vr+wq-x_G\left(q^2+r^2\right)+y_G\left(pq-\dot{r}\right)+z_G\left(pr+\dot{q}\right)\right]\\
Y &= m\left[\dot{v}-wp+ur-y_G\left(r^2+p^2\right)+z_G\left(qr-\dot{p}\right)+x_G\left(qp+\dot{r}\right)\right]\\
Z &= m\left[\dot{w}-uq+vp-z_G\left(p^2+q^2\right)+z_G\left(rp-\dot{q}\right)+y_G\left(rp+\dot{p}\right)\right]\\
K &= I_x\dot{p}+\left(I_z-I_y\right)qr+m\left[y_G\left(\dot{w}+vp-qu\right)-z_G\left(\dot{v}+ur-wp\right)\right]\\
M &= I_y\dot{q}+\left(I_x+I_y\right)rp+m\left[z_G\left(\dot{u}+wq-vr\right)-x_G\left(\dot{w}+vp-uq\right)\right]\\
N &= I_z\dot{r}+\left(I_y-I_x\right)pq+m\left[x_G\left(\dot{v}+ur-wp\right)-y_G\left(\dot{u}+wq-vr\right)\right]
\end{aligned}
\tag{1}
$$

movement of a spherical robot in water can be regarded as the response of a six-degree-of-freedom rigid body to various external forces. Equation (1) is the space motion equation of the spherical underwater robot.

Where m is the mass of the underwater robot. x_G, y_G, and z_G are the coordinates of the center of gravity of the robot. I_x, I_y and I_z are the moments of inertia of mass m for each coordinate axis. X, Y, Z are force of the robot, and K, M, N are torque of the robot. It can be seen from Equation (1) that there is cross-coupling between six degrees of freedom, which is one of the difficulties in underwater robot control. Table 1 shows the projections of velocity V, external force F, etc. in the motion coordinate system. The components of velocity and force are oriented in the direction of the coordinate axis, and the positive direction of angular velocity and moment is determined by the right-hand rule.

TABLE I. THE PARAMETERS OF THE SPHERICAL UNDERWATER ROBOT

Vector	X axis	Y axis	Z axis
Speed V	μ	v	ω
Angular velocity	p	q	r
Force	X	Y	Z
Torque	K	M	N

B. *Analysis of the Equation of Motion*

In order to simplify the problem, therefore, we only discuss the equations of motion for the horizontal and the vertical planes. According to the characteristics of the spherical underwater robot under water, the hydrodynamic Equation (2) and (3) of the vertical plane and the horizontal plane are obtained respectively. Next we take the transfer function in the dive process as an example for analysis.

$$
\begin{cases}
X = X_{\dot{u}}\dot{u}+X_{uu}u^2+X_{vv}v^2+X_{rr}r^2+X_{vr}vr\\
Y = Y_{\dot{v}}\dot{v}+Y_{\dot{r}}\dot{r}+Y_v v+Y_r r+Y_{v|v|}v|v|+Y_{v|r|}v|r|+Y_{r|r|}r|r|\\
N = N_{\dot{v}}\dot{v}+N_{\dot{r}}\dot{r}+N_v v+N_r r+N_{v|v|}v|v|+N_{v|r|}v|r|+N_{r|r|}r|r|
\end{cases}
\tag{2}
$$

$$
\begin{cases}
X = X_{\dot{u}}\dot{u}+X_{uu}u^2+X_{ww}w^2+X_{qq}q^2+X_{wq}wq\\
Z = Z_0+Z_{\dot{w}}\dot{w}+Z_{\dot{q}}\dot{q}+Z_w w+Z_{|w|}|w|+Z_q q+Z_{|w|w}w|w|+\\
Z_{ww}w^2+Z_{w|q|}w|q|+Z_{q|q|}q|q|\\
M = M_0+M_{\dot{w}}\dot{w}+M_{\dot{q}}\dot{q}+M_w w+M_{|w|}|w|+M_q q+\\
M_{|w|w}w|w|+M_{ww}w^2+M_{w|q|}w|q|+M_{q|q|}q|q|
\end{cases}
\tag{3}
$$

Here we do not consider the coupling of the horizontal and vertical planes, ignoring the nonlinear hydrodynamic term. When the robot performs vertical plane motion, it satisfies v=p=r=0, and the center of gravity x_g=0. Equation (4) represents the vertical plane linear dynamic equation, which can be obtained from Equation (1) to (3).

$$
\begin{aligned}
&\left(m-Z_{\dot{w}}\right)\dot{w}-Z_w w-Z_{\dot{q}}\ddot{\theta}-\left(mU+Z_q\right)\dot{\theta}=T_z\\
&\left(I_y-M_{\dot{q}}\right)\ddot{\theta}-M_q\dot{\theta}-M_\theta\theta-M_{\dot{w}}\dot{w}-M_w w=M_{T_z}
\end{aligned}
\tag{4}
$$

h is the distance from the center of gravity to the center of the float.Where is $\ddot{\theta}=\dot{q}$, $\dot{\theta}=q$, $u=U$, M_θ = -mgh . Simplification can obtain the linear equation Equation (5) of single state variables.

$$
\begin{aligned}
&A_3\dddot{w}+A_2\ddot{w}+A_1\dot{w}+A_0 w=\left(mx_g+Z_q\right)\ddot{M}_{T_z}+\\
&\left(mU+Z_q\right)\dot{M}_{T_z}+\left(I_{yy}-M_{\dot{q}}\right)\ddot{T}_z-M_\theta T_z
\end{aligned}
\tag{5}
$$

Considering $M_{\dot{q}}$, $Z_{\dot{q}}$ and $M_{\dot{w}}$ is small and negligible. And assumes that the center of gravity and the center of buoy are at one point, I_y=0. So we can get the transfer function in the dive process as Equation (6).

$$
\frac{W(s)}{T_z(s)}=\frac{I_y s^2-M_q s-M_\theta}{A_3 s^3+A_2 s^2+A_1 s+A_0}
\tag{6}
$$

Where $A_0=M_\theta Z_\omega$, $A_1=M_q Z_\omega-M_\theta(m-Z_{\dot{\omega}})-M_w(mU+Z_q)$, $A_2=-M_q(m-Z_{\dot{\omega}})-I_{yy}Z_\omega$, and $A_4=I_{yy}(m-Z_{\dot{\omega}})$. The spherical underwater robot has almost no change in the pitch angle in the vertical motion, and we can further simplify the Equation (6). We can also derive the dynamic equation of the horizontal plane in this way.

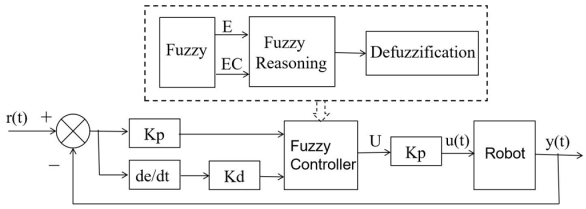

Fig. 2 The structure diagram of the fuzzy PD controller.

III. DESIGN OF FUZZY PD CONTROLLER

The dynamics of a spherical underwater robot is nonlinear. Due to the influence of uncertain factors such as currents, the hydrodynamic coefficient is difficult to estimate accurately or determined by experiments. And the coupling between degrees of freedom is also difficult to describe[15]. Considering the time-varying behavior of spherical underwater robots and the complexity and uncertainty of the environment, this paper adopts fuzzy PD control, which is more suitable for the underwater environment.

A. The Principle of Fuzzy Logic

The fuzzy control system is mainly composed of fuzzification, fuzzy reasoning and anti-fuzzification. The fuzzy control system is mainly composed of fuzzification, fuzzy reasoning and anti-fuzzification[16, 17]. The design principle of the fuzzy PD controller is mainly determined by the characteristics and performance of the spherical underwater robot. We then control the output of the system to achieve steady state requirements by adjusting the rate of deviation and deviation. The structure diagram of the fuzzy PD controller is shown in Fig. 2.

The input of the fuzzy control system is e, ec, and the output is u. In this paper, the range of the domain e is [-2m, 2m], the domain ec is [-2m/s, 2m/s], and the domain u is [-15º, 15º]. The membership function of the input variable and the output variable is shown in Fig. 3. The shape of the membership function has a great influence on the control effect. In order to improve the sensitivity and control characteristics, the triangular membership function is adopted.

When the deviation is large, we should quickly adjust the change strain of the control amount. When the deviation is small, in addition to eliminating the deviation, we should also consider the stability of the system which can prevent the system from overshooting[18]. Based on these principles, we

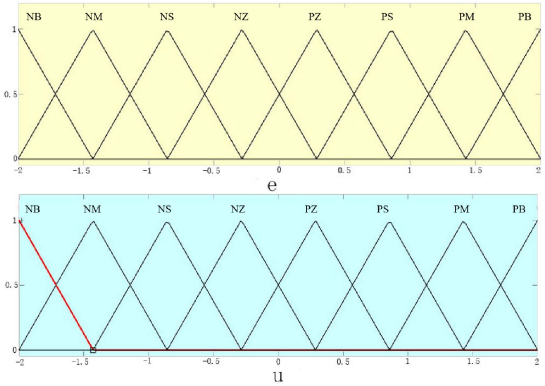

Fig. 3 The membership function of input variables e and output variables u. structure diagram of the fuzzy PD controller.

generated a fuzzy control table, as shown in Table 2.

When the deviation is large, we should quickly adjust the change strain of the control amount. When the deviation is small, in addition to eliminating the deviation, we should also consider the stability of the system which can prevent the system from overshooting. Based on these principles, we generated a fuzzy control table, as shown in Table 2.

TABLE II. FUZZY RULE TABLE

u		EC							
		NB	NM	NS	NZ	PZ	PS	PM	PB
E	NB	NB	NB	NM	NM	NS	NS	NZ	NZ
	NM	NB	NB	NM	NM	NS	NS	NZ	NZ
	NS	NB	NB	NM	NS	NS	NZ	NZ	NZ
	NZ	NB	NM	NM	NZ	NS	NZ	PM	PM
	PZ	NM	NM	PZ	PX	PZ	PM	PM	PB
	PS	PZ	PZ	PZ	PS	PS	PM	PB	PB
	PM	PZ	PZ	PS	PS	PM	PM	PB	PB
	PB	PZ	PZ	PS	PS	PM	PM	PB	PB

According to the fuzzy control table, we summarize 64 fuzzy rules. The format of the fuzzy rule is shown in Equation (7).

$$if\,(e\ is\ \mathrm{NB})\ \mathrm{and}\ (\mathrm{ec\ is\ NB})\ \mathrm{then}\ (\mathrm{u\ is\ NB}) \quad (7)$$

Next, Fuzzy reasoning is the core component of fuzzy controller, which is an approximate reasoning. In this paper,

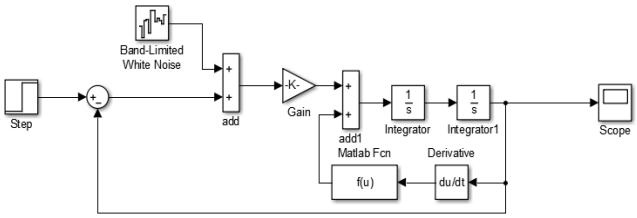

Fig. 4 The Simulink simulation diagram of hover motion without fuzzy PD control algorithm.

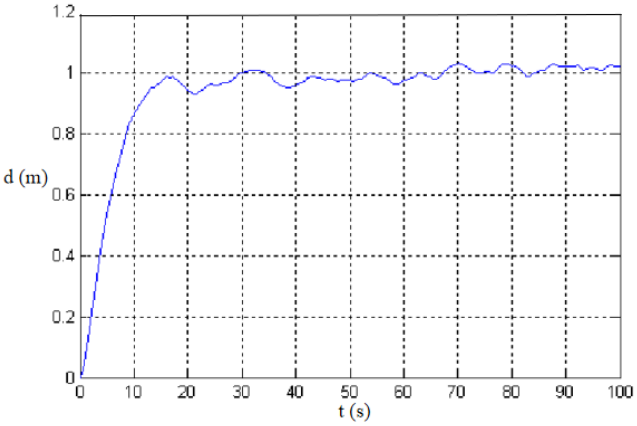

Fig. 5 Hover motion simulation results without without fuzzy PD control algorithm .

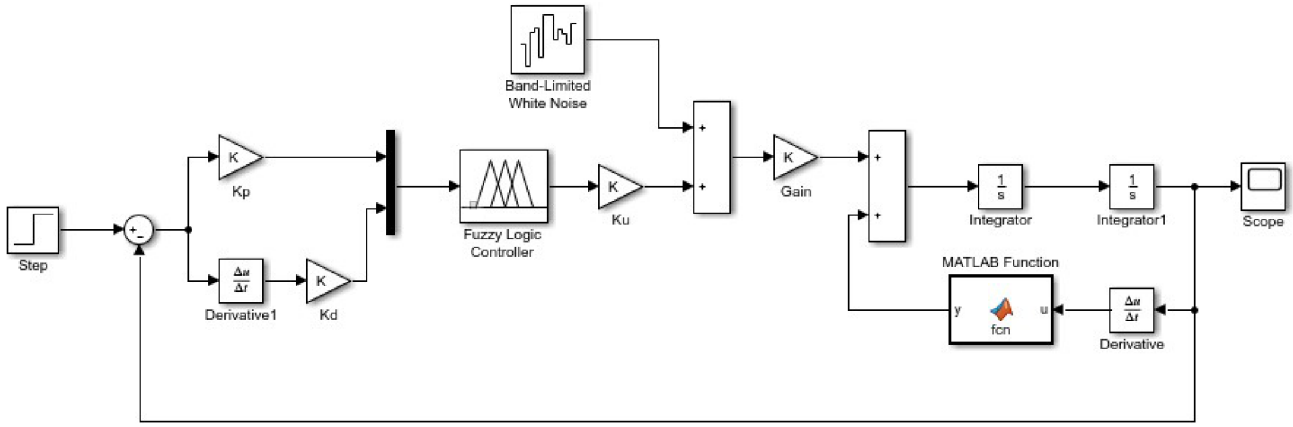

Fig. 6 The Simulink simulation diagram of hover motion with fuzzy PD control algorithm.

we use the Madanie method to convert the amount of blur produced into an accurate quantity, and the center of gravity method is as shown in Equation (8).

$$Z_0 = \frac{\int z \cdot u_N(z)dz}{\int u_N(z)dz} \tag{8}$$

In the formula, "∫"represents the algebraic integral of all membership values on the continuous domain, and $u_N(z)$ represents the membership function of input variable, and z represents the center of gravity of the area corresponding to the membership function of output variable.

B. *Hover Control Simulation Model*

For nonlinear systems, where the coupling is not dominant, and without the trim control, this method greatly simplifies the design of the controller[19]. The fuzzy PD controller has strong adaptability and can overcome the uncertainty of the marine environment. In the dive process of the spherical underwater robot, the moving speed is low, and the coupling between the motion states can be ignored.

To verify the effectiveness of the proposed method, we first carried out the hover experiments based on the fuzzy controller, and simulated it in Matlab. The Simulink simulation model is shown in Fig. 4.

Then adjust the gain coefficient of the fuzzy controller appropriately to obtain the system response curve as shown in Fig. 5. In Fig. 5, we set the mass m to 2.25kg, diving depth to 1 meter, and to better simulate the sea state, we added white noise interference during the simulation.

From the fuzzy control results, we can see that the fuzzy controller output has a relatively serious phase lag, and the response tracking of the control system is poor. So we joined the PD control for optimization. The Simulink simulation model is shown in Fig. 6. The fuzzy control system editor in Matlab is used to determine the input and output variable domain and membership function. After the gain adjustment, the corresponding system response curve is obtained, as shown in Fig. 7.

In Fig. 7, we also set the diving depth to 1 meter, which is convenient for comparison with fuzzy control. It can be seen from the simulation results that after adding PD control, the

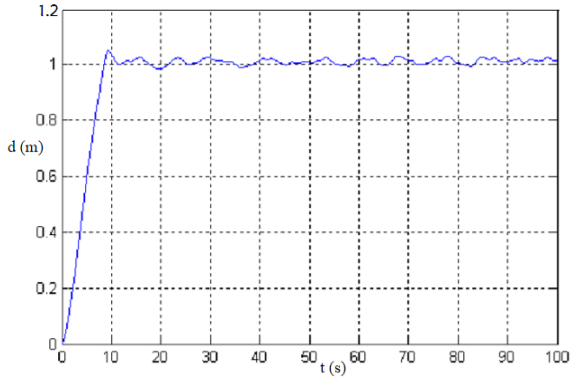

Fig. 7 Hover motion simulation result with fuzzy PD controller.

system solves the problem of phase lag and the tracking effect is more stable. The simulation results showed that the control method had a good control effect on nonlinear systems, and met the control requirements of the spherical underwater robot in the dive process.

IV. Underwater Experiments And Data Processing

We use the spherical underwater robot as an experimental platform to complete underwater hovering experiments. Before the experiment, we first adjusted the robot's own counterweight and the jet motor thrust problem, so that the robot can float in the water.

A. *Data Processing Method for NDI System*

The robot uses the NDI optical tracking system to collect data during the underwater sinking process. The tracking system is 80cm away from the ground, and the acquisition

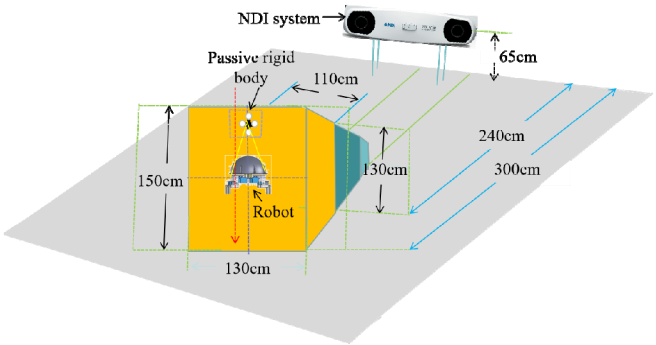

Fig. 8 The principle of NDI tracking system data acquisition.

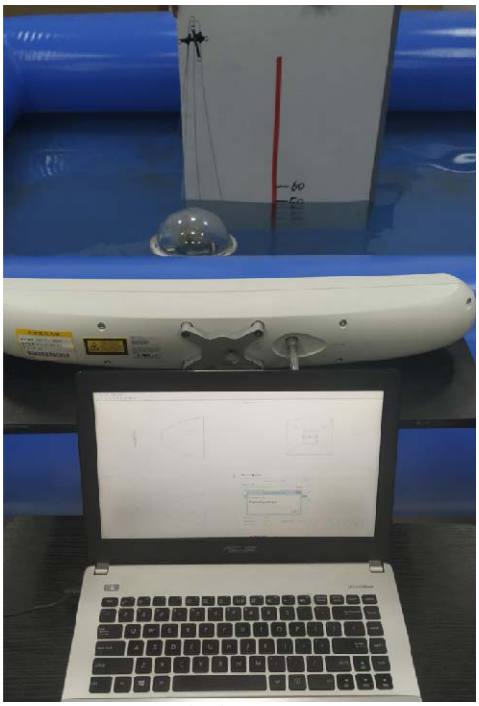

depth = 0 mm

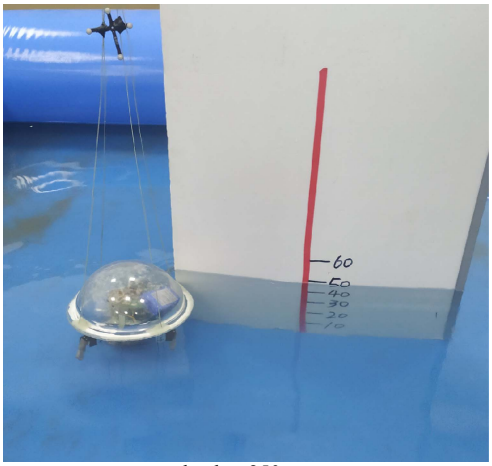

depth = 250 mm

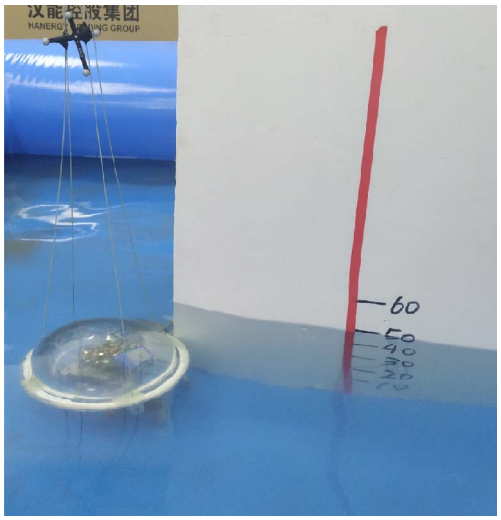

depth = 500 mm

Fig. 9 Sinking motion state of the spherical underwater robot.

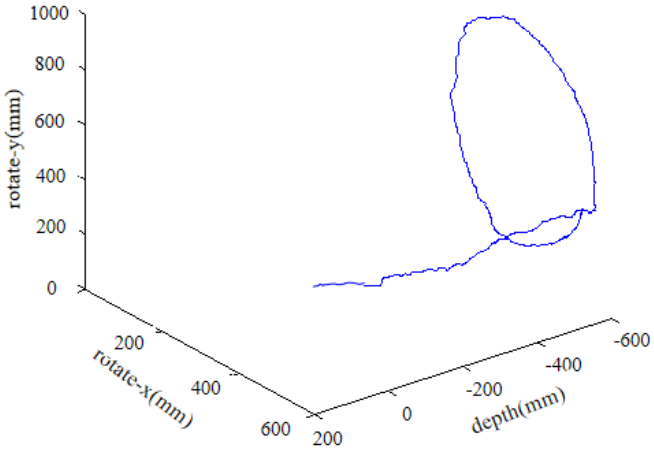

Fig. 10 The result of spherical underwater robot motion data acquisition.

principle is shown in Fig. 8. We fixed the acquisition device to the robot. When starting the dive, the NDI system began recording the data of the spherical underwater robot.

B. Experiments of Hover Motion

During the sinking process of the spherical underwater robot, we completed the hover motion experiments of the robot at the depth of 0 mm, 250 mm and 500 mm respectively. When the robot reaches the target position, the robot will perform a rotary motion, which facilitates the observation and recording of data. The dive state of the spherical underwater robot is shown in Fig. 9.

Most of the data in the experiment was measured at 70% to 90% power, and we measured a maximum thrust of 16 pounds. We use the NDI system for data acquisition and processing. The acquisition device is fixed to the robot through the bracket, thus ensuring the accuracy and stability of data acquisition. But this is limited to measurements in shallow waters. We will process and analyze the data when the robot sinks to 0.5 meters. The processing result is shown in Fig. 10. Includes sinking and rotating motion. 0mm to -500mm indicates the dive distance of the robot, which is indicated by h in the Fig. 10. The robot dive from 0 cm to 50 cm, and then rotate. The rotational motion is represented by rotate-x and rotate-y in the Fig. 10, rotate-x and rotate-y indicate the reference plane when the robot rotates. And starts to rotate when the robot reaches -500 mm. We can see from the figure that the robot's motion trajectory is close to a straight line. Since the robot motion is not directional, the actual trajectory has a certain deviation from the ideal trajectory. When the robot reaches the specified position, the robot will rotate, which is affected by the water wave during rotation, which causes the robot's motion trajectory to deviate from the ideal trajectory. However, the overall error is not more than 5%. The experimental results further verify the validity and practicability of the fuzzy PD control algorithm.

The NDI system collects data through its own coordinates (tool coordinate system), which has high measurement accuracy. The tool coordinate system has its own coordinate system, so the measured coordinate axes will differ from the physical coordinate axes.

C. Discussion

When conducting underwater experiments, sometimes the experiment did not achieve satisfactory results due to problems with the model and the external environment. Due to the limitations of the experimental conditions (the shallow depth of the pool and the narrow width), the robot is not easy to move according to the predetermined trajectory. The spherical underwater robot cannot move according to the predetermined trajectory, and mainly has the following influencing factors.

Water Wave: When the robot moves underwater, it will generate large water waves. The fluctuation of water affects the stability of the spherical underwater robot. In this case, the robot is less likely to achieve directional motion, so try to ensure no fluctuations during testing.

Human Factors: In short-distance measurement, the artificially determined time error is particularly large. In addition, the robot does not move along a straight line, and in most cases moves along a curve.

Objective Factors: The robot is also affected by various factors during the movement, which makes the measurement results have errors. For example, speed has a greater impact on locating.

V. Conclusion

In this paper, according to the dynamic equation, we solved the transfer function of the spherical underwater robot in the dive process, which provided stability for the hover motion of the spherical underwater robot. Next, we designed the fuzzy PD controller, and used the Simulink platform to build two hover motion simulation models, including using fuzzy PD controller and without fuzzy PD controller. In the simulation experiments, we verified the effectiveness of the fuzzy PD controller by adding 5% Gaussian white noise. Finally, we carried out the hover motion experiments and analyzed the experimental data. The experimental results showed that the fuzzy PD controller had better self-adjusting ability. In the future, we will complete the hover motion experiments in deep water.

Acknowledgment

This research is supported by National Natural Science Foundation of China (61703305), Key Research Program of the Natural Science Foundation of Tianjin (18JCZDJC38500) and Innovative Cooperation Project of Tianjin Scientific and Technological (18PTZWHZ00090).

References

[1] Hakan Acikgoz, Resul Coteli, Besir Dandil and Fikret Ata, "Experimental evaluation of dynamic performance of three-phase AC-DC PWM rectifier with PD-type-2 fuzzy neural network controller," *Iet Power Electronics*, vol. 12, no. 4, pp. 693-702, 2019.

[2] Ali Alouache and Qinghe Wu, "Fuzzy logic PD controller for trajectory tracking of an autonomous differential drive mobile robot (i.e. Quanser Qbot)," *Industrial Robot-the International Journal of Robotics Research and Application*, vol. 45, no. 1, pp. 23-33, 2018.

[3] B. Braginsky and H. Guterman, "Obstacle Avoidance Approaches for Autonomous Underwater Vehicle: Simulation and Experimental Results," *Ieee Journal of Oceanic Engineering*, vol. 41, no. 4, pp. 882-892, 2016.

[4] X. Cao, C. Y. Sun and M. Z. Chen, "Path planning for autonomous underwater vehicle in time-varying current," *Iet Intelligent Transport Systems*, vol. 13, no. 8, pp. 1265-1271, 2019.

[5] Y. T. Chen, W. Wang, L. Li, R. Kelly and G. M. Xie, "Obstacle effects on electrocommunication with applications to object detection of underwater robots," *Bioinspiration & Biomimetics*, vol. 14, no. 5, pp. 15, 2019.

[6] Yufeng Chen, Neel Doshi, Benjamin Goldberg, Hongqiang Wang and Robert J. Wood, "Controllable water surface to underwater transition through electrowetting in a hybrid terrestrial-aquatic microrobot," *Nature Communications*, vol. 9, no. 1, pp. 2495-2505, 2018.

[7] Guo J , Wu G , Guo S, "Fuzzy PID algorithm-based motion control for the spherical amphibious robot," *IEEE International Conference on Mechatronics & Automation*, pp. 1583-1588, 2015.

[8] Shuxiang G , Shaowu P , Liwei S, "Visual Detection and Tracking System for a Spherical Amphibious Robot," *Sensors*, vol. 17, no. 4, pp. 870-890, 2017.

[9] He Y , Zhang X , Dong M, "Performance evaluation of spherical robot for amphibious applications," *Microsystem Technologies*, vol. 25, no. 12, pp. 4483-4494, 2019.

[10] Sadegh Etedali and Saeed Tavakoli, "PD/PID Controller Design for Seismic Control of High-Rise Buildings Using Multi-Objective Optimization: A Comparative Study with LQR Controller," *Journal of Earthquake and Tsunami*, vol. 11, no. 3, pp. 1750009, 2017.

[11] Mohammad Reza Gharib and Armin Daneshvar, "Quantitative-fuzzy Controller Design for Multivariable Systems with Uncertainty," *International Journal of Control Automation and Systems*, vol. 17, no. 6, pp. 1515-1523, 2019.

[12] Zheng L, Guo S, Gu S, "The communication and stability evaluation of amphibious spherical robots," *Microsystem Technologies*, vol. 25, no. 7, pp. 2625-2636, 2019.

[13] He Y, Zhu L, Sun G, "Study on formation control system for underwater spherical multi-robot," Microsystem Technologies, vol. 25, no. 68, pp. 253-262, 2018.

[14] Zhang W , Dong X , Liu X, "Switched Fuzzy-PD Control of Contact Forces in Robotic Microbiomanipulation," *IEEE Transactions on Biomedical Engineering*, vol. 64, no.5, pp. 1169-1177, 2017.

[15] Vishal Goyal, Puneet Mishra, Aasheesh Shukla, Vinay Kumar Deolia and Aarti Varshney, "A fractional order parallel control structure tuned with meta-heuristic optimization algorithms for enhanced robustness," *Journal of Electrical Engineering-Elektrotechnicky Casopis*, vol. 70, no. 1, pp. 16-24, 2019.

[16] C. Greatwood and A. G. Richards, "Reinforcement learning and model predictive control for robust embedded quadrotor guidance and control," *Autonomous Robots*, vol. 43, no. 7, pp. 1681-1693, 2019.

[17] Y. L. Hernandez, O. G. Frias, N. Lozada-Castillo and A. L. Juarez, "Control Algorithm for Taking off and Landing Manoeuvres of Quadrotors in Open Navigation Environments," *International Journal of Control Automation and Systems*, vol. 17, no. 9, pp. 2331-2342, 2019.

[18] Y. Q. Jiang, Y. Li, Y. M. Su, Z. Y. Zhou, T. Ma, L. An and J. Y. He, "Route optimizing and following for autonomous underwater vehicle ladder surveys," *International Journal of Advanced Robotic Systems*, vol. 15, no. 6, pp. 16, 2018.

[19] M. Reyasudin Basir Khan, Jagadeesh Pasupuleti and Razali Jidin, "Load frequency control for mini-hydropower system: A new approach based on self-tuning fuzzy proportional-derivative scheme," *Sustainable Energy Technologies and Assessments*, vol. 30, pp. 253-262, 2018.